

Evaluation of the Daylight Cycle of Model-Predicted Cloud Amount and Condensed Water Path over Europe with Observations from MSG SEVIRI

R. A. ROEBELING AND E. VAN MEIJGAARD

Royal Netherlands Meteorological Institute, De Bilt, Netherlands

(Manuscript received 20 December 2007, in final form 18 June 2008)

ABSTRACT

The evaluation of the diurnal cycle of cloud amount (CA) and cloud condensed water path (CWP) as predicted by climate models receives relatively little attention, mostly because of the lack of observational data capturing the diurnal cycle of such quantities. The Spinning Enhanced Visible and Infrared Imager (SEVIRI) onboard the geostationary *Meteosat-8* satellite is the first instrument able to provide accurate information on diurnal cycles during daylight hours of cloud properties over land and ocean surfaces. This paper evaluates the daylight cycle of CA and CWP as predicted by the Regional Atmospheric Climate Model version 2 (RACMO2), using corresponding SEVIRI retrievals. The study is done for Europe using hourly cloud properties retrievals from SEVIRI during the summer months from May to September 2004.

The results of this study show that SEVIRI-retrieved daylight cycles of CA and CWP provide a powerful tool for identifying climate model deficiencies. Over Europe the SEVIRI retrievals of cloud condensed water paths comprise about 80% liquid water and about 20% ice water. The daylight cycles of CA and CWP from SEVIRI show large spatial variations in their mean values and time of daily maximum and daytime-normalized amplitude. In general, RACMO2 overestimates CWP by about 30% and underestimates CA by about 20% as compared to SEVIRI. The largest amplitudes are observed in the Mediterranean and northern Africa. For the greater part of the ocean and coastal areas the time of daily maximum CWP is found during morning, whereas over land this maximum is found after local solar noon. These features are reasonably well captured by RACMO2. In the Mediterranean and continental Europe RACMO2 tends to predict maximum CWP associated with convection to occur about two hours earlier than SEVIRI indicates.

1. Introduction

The representation of diurnal variations in cloud parameters by present-day climate models is relatively poor and, therefore, limits the predictability of cloud feedbacks in a changing climate (Duynderke et al. 2004; Lenderink et al. 2004). During the past decade, the focus has been on modeling climate change and variability on interseasonal to interannual time scales (e.g., Ramaswamy et al. 2001). This requires the mean model output to be accurate over periods of at least one month, whereas the representation of the diurnal variations is less relevant for this application. However, information on the behavior of the diurnal cycle of cloud parameters allows the evaluation of models on time scales typical for atmospheric physical processes, like convection and the formation of clouds and precipitation. As such, it may

contribute to identifying the processes that may be responsible for systematic model errors. Thus, the evaluation of diurnal cycles of model-predicted cloud properties may help to improve the parameterization of cloud processes and increase the confidence in climate and numerical weather prediction models.

Cloud condensed water path (CWP) and cloud amount (CA) exhibit marked diurnal cycles, which behave differently in different climate regions and over land and ocean surfaces. Cloud condensed water path is defined as the sum of cloud liquid water path (LWP) and cloud ice water path (IWP). In several studies, satellite measurements have been used to describe the diurnal cycle of LWP. For clouds over subtropical and tropical oceans, Wood et al. (2002) showed from Tropical Rainfall Measuring Mission (TRMM) Microwave Imager (TMI) observations that the amplitude of the diurnal cycle of LWP is a considerable fraction of the mean (about 50%) and that the maximum LWP occurs in early morning. This is consistent with the daytime variations in LWP values of marine stratocumulus

Corresponding author address: R. A. Roebeling, P.O. Box 201, KNMI, 3730 AE De Bilt, Netherlands.
E-mail: roebelin@knmi.nl

clouds as observed from the Geostationary Operational Environment Satellite (GOES) by Greenwald and Christopher (1999). Finally, a study by Fairall et al. (1990) found even larger diurnal cycles in LWP (70%) from ground-based microwave radiometer (MWR) measurements for the San Nicolas Islands southwest of Los Angeles, California.

The LWP can be retrieved with good accuracy from ground-based MWR measurements, but the number of measurement sites is insufficient to capture the spatial and temporal variations in LWP values observed from satellites (Rossow and Cairns 1995). Over the ocean, microwave imagers such as TMI or the Special Sensor Microwave Imager (SSM/I) are a means to retrieve LWP (Weng et al. 1997; Wood et al. 2002). In addition, various methods have been developed to retrieve CWP from satellite measurements. Passive imagers, such as the Advanced Very High Resolution Radiometer (AVHRR) on board NOAA satellites, are one way to retrieve CWP over land and ocean surfaces. The principle of these retrieval methods is that the reflection of radiation by clouds in the nonabsorbing visible channels (0.6 or 0.8 μm) is primarily a function of the cloud optical thickness, while the reflection at the water (or ice) absorbing near-infrared channels (1.6, 2.1, or 3.8 μm) is primarily a function of cloud particle size (Nakajima and Nakajima 1995; Platnick et al. 2003; Roebeling et al. 2006a). The CWP is then determined as the product of the cloud optical thickness and the effective radius of the water droplets or ice crystals (King et al. 2004; Rossow and Schiffer 1999; Roebeling et al. 2006a).

In recent years good progress has been made in quantifying the accuracy of the fraction of condensed water that is identified as liquid water in the retrievals from passive imagers. Several studies compared ground-based LWP retrievals from MWRs with LWP retrievals from the NOAA AVHRR (Han et al. 1995; Jolivet and Feijt 2005) and the Spinning Enhanced Visible and Infrared Imager (SEVIRI) on board *Meteosat-8* (Roebeling et al. 2008). These studies found that the accuracies (biases) of the satellite-retrieved LWP values vary between 5 and 15 g m^{-2} . The precision (standard error) of these retrievals is better than 30 g m^{-2} for thin clouds, whereas lower precision is found for thick clouds (up to 100 g m^{-2}). The accuracy of climate and numerical weather model-predicted LWP values is found to be considerably lower than those from satellite or ground-based MWR observations. During the First International Satellite Cloud Climatology Project (ISCCP) Regional Experiment (FIRE) Arctic Cloud Experiment, Curry et al. (2000) compared large-scale model LWP values to MWR-inferred LWP values. They found that all models underestimate the mean

LWP value by 20–30 g m^{-2} , which corresponds to relative differences larger than 60% for the Arctic. For nonprecipitating water clouds, van Meijgaard and Crewell (2005) found that MWR-observed and model-predicted LWP values differ by up to 50 g m^{-2} in their mean values. Accurate representation of the diurnal cycle of CA and LWP within numerical weather and climate prediction models is even more difficult. Duynderke et al. (2004) evaluated the diurnal cycles of CA and LWP for stratocumulus clouds for 10 of these models. They found that more than half of the models predicted too thin cloud layers with much weaker (20%–50%) diurnal cycles of LWP than those observed by MWR. The inadequate parameterization of the entrainment rate in stratocumulus-topped boundary layers was given as main reason for the observed differences. For shallow cumulus over land, Lenderink et al. (2004) found that single-column-model (SCM) versions have too high CA and LWP values in the afternoon as compared to large-eddy simulation models. Analysis of model results showed that in most SCM integrations the clouds did not dissolve at the end of the daytime period.

To date there is much uncertainty about the accuracy of the fraction of condensed water that is identified as ice water in the retrievals from passive imagers. The methods that have been developed to retrieve IWP from ground-based measurements are either only applicable to thin cirrus clouds or not accurate enough for validation studies. Illingworth et al. (2007) found that the methods based on radar reflectivities and lidar backscatter observations (van Zadelhoff et al. 2007; Donovan 2003) are accurate but only applicable to thin cirrus clouds ($\text{IWP} < 50 \text{ g m}^{-2}$). On the other hand, the methods that can be applied to thick cirrus clouds, such as the radar reflectivity and temperature method proposed by Hogan et al. (2006), have low precision ($\sim 50\%$). In the future, the combined use of observations from active satellite instruments, such as Cloudsat and Cloud–Aerosol Lidar and Infrared Pathfinder Satellite Observation (CALIPSO), may be the best way forward to access the accuracy of IWP values for cirrus clouds. In the case of frontal systems or deep convective systems, clouds are often of mixed phase and have generally large CWP values ($\text{CWP} > 150 \text{ g m}^{-2}$). For these systems retrievals from active satellite or ground-based instruments remain of little value for providing IWP validation data. Although direct validation of IWP is cumbersome, the relationship between cloud optical thickness and effective radius is valid for both liquid water and ice water clouds.

Relatively little attention has been given to the evaluation of regional variations in the representation of the diurnal cycle of CWP by numerical weather and climate prediction models. Accurate information on

these diurnal cycles over land and ocean would provide a key test of many aspects in the physical parameterizations operated in these models, such as the representation of convection, turbulence, and cloud processes. For the first time, the SEVIRI instrument provides the opportunity to generate well-resolved diurnal cycles during daylight hours of CA and CWP over land and ocean surfaces. SEVIRI operates 11 spectral channels, at a sampling frequency of 15 min and a spatial resolution of $3 \times 3 \text{ km}^2$ at nadir, and one high-resolution visible channel ($1 \times 1 \text{ km}^2$). These specifications are superior to, for example, GOES, which operates five channels at a sampling frequency of 30 min and a spatial resolution of $3 \times 3 \text{ km}^2$ at nadir and one high-resolution visible channel ($1 \times 1 \text{ km}^2$). The purpose of this study is to evaluate diurnal cycles during daylight hours, hereafter referred to as daylight cycles, of CA and CWP from the Regional Atmospheric Climate Model, version 2 (RACMO2) (Lenderink et al. 2003; de Bruijn and van Meijgaard 2005) with corresponding daylight cycles derived from SEVIRI. The study area covers large parts of Europe and comprises land and ocean surfaces within various climate regions. The CA and CWP values are retrieved with the cloud physical properties (CPP) algorithm developed at the Royal Netherlands Meteorological Institute (KNMI) within the Climate Monitoring Satellite Application Facility (CM-SAF) of the European Organization for the Exploitation of Meteorological Satellites (EUMETSAT) (Roebeling et al. 2006a). To investigate whether SEVIRI retrieves realistic LWP values we have compared them with observations inferred from ground-based MWR measurements. The evaluation of RACMO2-predicted daylight cycles of CA and CWP with SEVIRI observations over Europe is carried out by comparing the summer-months mean, the daytime-normalized amplitude, and the time of the daily maximum. Finally, the daylight cycles of CA and CWP are evaluated in greater detail for three subdomains situated in Europe, each representing a climate zone.

The outline of this paper is as follows. In section 2, the ground-based and satellite measurement devices are described. The methods to retrieve cloud properties from ground-based and satellite observations and to predict cloud parameters with models are presented in section 3. In section 4, LWP predictions from RACMO2 are compared against the LWP retrievals from MWRs and SEVIRI at Palaiseau, France, and Chilbolton, United Kingdom. The regional evaluation of the daylight cycle of CA and CWP from RACMO2 with SEVIRI over Europe is presented in section 5. In section 6, the sensitivity of RACMO2-predicted CWP to model resolution and precipitation parameterization is

evaluated. Finally, in section 7, results are discussed in a broader context and conclusions are drawn.

2. Measurements

a. Ground-based observations

The ground-based cloud observations were collected in the framework of the Cloudnet project, which was a European Union-funded research project that has produced a database of cloud measurements for three cloud remote sensing stations (Illingworth et al. 2007). These stations are located at Cabauw, the Netherlands (51.97°N , 4.93°E), Chilbolton (51.14°N , 1.44°W), and Palaiseau (48.71°N , 2.21°E). The sites were equipped with radar, lidar, and a suite of passive instrumentation during the period from 2001 to 2004. The active instruments (lidar and cloud radar) provided detailed information on vertical profiles of the relevant cloud parameters, while dual-channel microwave radiometers provided information on LWP and integrated water vapor (IWV).

b. Satellite observations

Meteosat Second Generation (MSG) is a new series of European geostationary satellites operated by EUMETSAT. The first MSG satellite (*Meteosat-8*) was launched successfully in August 2002 and positioned at an altitude of about 36 000 km above the equator at 3.4°W . The SEVIRI instrument scans the complete disk of the earth every 15 min, and operates three channels at visible and near-infrared wavelengths between 0.6 and $1.6 \mu\text{m}$, eight channels at infrared wavelengths between 3.8 and $14 \mu\text{m}$, and one high-resolution visible channel. The nadir spatial resolution of SEVIRI is $1 \times 1 \text{ km}^2$ for the high-resolution channel, and $3 \times 3 \text{ km}^2$ for the other channels. Over northern Europe the spatial resolution of the visible, near-infrared, and infrared channels of SEVIRI reduces to about $4 \times 7 \text{ km}^2$. The SEVIRI data are made available for EUMETSAT users through the Unified Meteorological Archive and Retrieval Facility (UMARF) archive (<http://archive.eumetsat.org/umarf/>).

3. Methods

a. LWP retrieval from ground-based observations

Passive microwave radiometers measure brightness temperature at different frequencies that have distinct atmospheric absorption characteristics. The MWRs operated at the Cloudnet sites measure brightness temperatures at frequencies near 23 and 30 GHz, which are used for the simultaneous retrieval of LWP and IWV (Gaussiat et al. 2007). The retrieval of LWP is done in a

two-step approach. First, two independent equations are used to link the optical depths, derived from the brightness temperatures, to IWV for clear-sky or ice-only conditions, and then calculate the optical depth calibration factors for the considered frequencies. During these conditions, which are identified from independent lidar and radar observations, the LWP values are assumed to be zero (van Meijgaard and Crewell 2005). Second, during cloudy periods LWP and IWV are calculated from two equations that relate the observed optical depth to LWP, IWV, mass absorption of liquid, mass absorption of vapor, and a calibration factor. The retrieval algorithm corrects for variations in the coefficients of mass absorption of liquid and mass absorption of vapor. The algorithms use lidar cloud altitude observations combined with pressure, temperature, and humidity profiles predictions from a numerical weather prediction model to predict the correction coefficients. The retrieval of LWP from MWR is strongly disturbed by rainfall since the instrument antenna or radiometer can become covered by water droplets or a thin water layer. Moreover, none of the MWRs are sensitive to ice clouds because ice crystals do not contribute to the MWR radiances at the probed frequencies. The two-channel MWRs operated at Chilbolton and Palaiseau have an estimated accuracy of about 5 g m^{-2} and precision of about 15 g m^{-2} (Gaussiat et al. 2007).

b. Cloud amount and condensed water path retrievals from SEVIRI

The CPP algorithm of the CM-SAF is used to retrieve CWP from SEVIRI reflectance at 0.6 and 1.6 μm (Roebeling et al. 2006a). For cloudy pixels, the CPP algorithm retrieves cloud optical thickness, particle size, and cloud phase in an iterative manner by simultaneously comparing satellite-observed reflectance at visible (0.6 μm) and near-infrared wavelengths (1.6 μm) to lookup tables (LUTs) of simulated reflectance for given values of optical thickness, particle size, and surface albedo. The optical thicknesses range from 1 to 256. Particles of water clouds are assumed to be spherical droplets with effective radii between 1 and 24 μm . For ice clouds imperfect hexagonal ice crystals (Hess et al. 1998) are assumed with effective radii between 6 and 51 μm . The retrieval algorithm assigns the phase “ice” to pixels for which the 0.6- μm and 1.6- μm reflectances correspond to simulated reflectance of ice clouds and the cloud-top temperature is lower than 265 K. The remaining cloudy pixels are considered to represent water clouds. The validity of the cloud phase retrieval method is described by Wolters et al. (2008). Finally, CWP is computed from the retrieved cloud optical thickness (τ_{vis}) and effective radius (r_e) as follows (Stephens et al. 1978):

$$\text{CWP} = \frac{2}{3} \tau_{\text{vis}} r_e \rho_l, \quad (1)$$

where ρ_l is the density of liquid water and r_e the effective radius of either spherical water droplets or imperfect hexagonal ice crystals. The CPP algorithm applies the equation of Stephens et al. (1978) both to water and ice clouds, which is similar to the CWP retrieval methods of the Moderate Resolution Imaging Spectroradiometer (MODIS) (King et al. 2004) and the ISCCP (Rossow and Schiffer 1999).

The LUTs have been generated using the Doubling Adding KNMI (DAK) radiative transfer model (De Haan et al. 1987; Stammes 2001), while Scanning Imaging Absorption Spectrometer for Atmospheric Cartography (SCIAMACHY) spectra have been used to calculate the conversion coefficients between the simulated line reflectances of DAK and the observed SEVIRI channel reflectances. The surface reflectance maps have been generated from one year of MODIS white-sky albedo data. The algorithm to separate cloud-free from cloud-contaminated and cloud-filled pixels originates from the MODIS cloud detection algorithm (Ackerman et al. 1998; Platnick et al. 2003). It has been adapted for SEVIRI to account for differences in spectral channels and resolution and has been made independent from ancillary information on surface temperature or atmospheric profiles (J. Riédi 2007, personal communication).

The cloud properties retrievals are made available through the CM-SAF project. On their Web site (<http://www.cmsaf.eu>) daily, monthly, and monthly diurnal cycle data of SEVIRI and AVHRR cloud properties can be ordered. The hourly cloud properties retrievals from SEVIRI can be provided by the Deutscher Wetterdienst (DWD) on special request.

c. RACMO2 integrations

RACMO2 is a hydrostatic limited-area model used for regional climate modeling (Lenderink et al. 2003). The model has been developed at KNMI by porting the physics package of the European Centre for Medium-Range Weather Forecasts Integrated Forecasting System (IFS), release cy23r4, into the forecast component of the High Resolution Limited Area Model (HIRLAM) numerical weather prediction model, version 5.0.6 (de Bruijn and van Meijgaard 2005). This release also served as the basis for the ECMWF Re-Analysis (ERA-40) project (Uppala et al. 2005). Cloud processes in RACMO2 are described by prognostic equations for cloud fraction and condensed water (liquid water and ice). The distinction between the liquid and the ice phase is made as a function of temperature. Cloud-forming and

cloud-dissolving processes are considered subgrid scale, and hence parameterized; however, large-scale transport of cloud properties is accounted for on the resolved scale. Sources and sinks of cloud fraction and cloud condensate are process oriented and physically based, in contrast to the more commonly applied statistical approach. Total 2D cloud cover is obtained from the vertical profile of cloud fraction by assuming random-maximum overlap within a model grid box. Details of the cloud parameterizations are described in White (2003, and references therein).

In this paper, we apply an upgraded version of RACMO2. Modifications relative to the previous version (Lenderink et al. 2003) are described by E. van Meijgaard et al. (2008). Of relevance to this work are the replacement of the cumulus convection scheme and the prognostic cloud scheme by versions from release cy28r1 of the ECMWF IFS. The upgrade was, in particular, motivated by the introduction in this release of an improved description of the convective triggering over land (Jakob and Siebesma 2003). The role of the new convection scheme is discussed in section 6. For the purpose of this study, RACMO2 is operated at a horizontal resolution of $25 \times 25 \text{ km}^2$ and a vertical mesh of 40 layers with the top layer at 10 hPa and the bottom layer at 10 m above the surface. The model domain, counting 206 points in the zonal direction and 224 points in the meridional direction, fully encloses the domain of evaluation. Short-term integrations of 36 h have been performed on a daily basis starting from the 1200 UTC ECMWF analysis. Forcings at the lateral boundaries are taken from subsequent ECMWF operational analyses of wind, temperature, and humidity at 6-h time intervals. At the surface, sea surface temperatures and sea ice fraction are prescribed from observations. To avoid spinup problems of cloud-related parameters output for the first 12 h of each hindcast is ignored.

4. Comparison of LWP values from MWR, SEVIRI, and RACMO2

SEVIRI-observed and RACMO2-predicted LWP values have been compared against corresponding MWR observations for the Cloudnet sites at Chilbolton and Palaiseau over the period from 15 May to 15 September 2004. RACMO2 output is made available at a temporal resolution of 1 h. Similarly, hourly SEVIRI data are processed with the CPP algorithm to obtain LWP values. The SEVIRI cloud property data are aggregated on the model resolution ($25 \times 25 \text{ km}^2$) to obtain satellite-inferred LWP data at model resolution. Because the CPP algorithm uses visible reflectance, the

retrievals are only made during daylight hours for solar zenith angles less than 72° .

The comparison of SEVIRI and RACMO2 with MWR is evidently restricted to a sample for which valid LWP observations could be retrieved from the MWR measurements. The sample includes LWP observations from MWR that are made during cloud free conditions, but is limited by rejecting those observations made in the presence of ice clouds or precipitating clouds overhead from the MWR. Ice clouds are excluded to obtain a sample of retrieved columnar values that solely comprise liquid water contributions. The presence of water clouds from the ground-based observations is diagnosed from the Cloudnet target categorization data (Illingworth et al. 2007). Rain gauge observations are used to identify MWR measurements that were contaminated by rainfall. Moreover, MWR observations with LWP values larger than 800 g m^{-2} are excluded. The LWP retrievals from MWR are averaged in a 64-min interval, which is considered a representative interval for estimating LWP values in a RACMO2 grid box. The RACMO2 samples have been divided into two groups in a similar manner, as described by van Meijgaard and Crewell (2005). The first group contains the liquid water samples of non-precipitating clouds. The second group contains the liquid water samples of both precipitating and non-precipitating clouds. The second group is included because convectively produced liquid water in RACMO2 will always be released as precipitation irrespective of the thickness of the convective layer. In total, the dataset of collocated and synchronized LWP values from MWR, SEVIRI, and RACMO2 comprises 486 cases at Chilbolton and 268 cases at Palaiseau for all water clouds and 349 cases at Chilbolton and 229 cases at Palaiseau for nonprecipitating water clouds.

To illustrate the effect of sampling time on the mean and median LWP values, Fig. 1 presents a comparison between MWR-retrieved LWP values averaged in intervals ranging from 1 to 256 min and SEVIRI-retrieved LWP values spatially aggregated at three different horizontal resolutions (4×7 , 25×25 , and $50 \times 50 \text{ km}^2$). This comparison was done for Chilbolton using the 0.5-min data from MWR and hourly data from SEVIRI during the four-month observation period. Because LWP is a quantity that can be averaged linearly, spatial or temporal averaging have little effect on the mean values. Therefore, the mean LWP value from MWR is hardly affected by increasing the sampling time from 1 to 256 min, while the mean LWP values from SEVIRI differ less than 2 g m^{-2} due to increasing the resolution from 4×7 to $50 \times 50 \text{ km}^2$. These results confirm that the resampling procedure is precise. The SEVIRI-calculated median LWP values retrieved at satellite

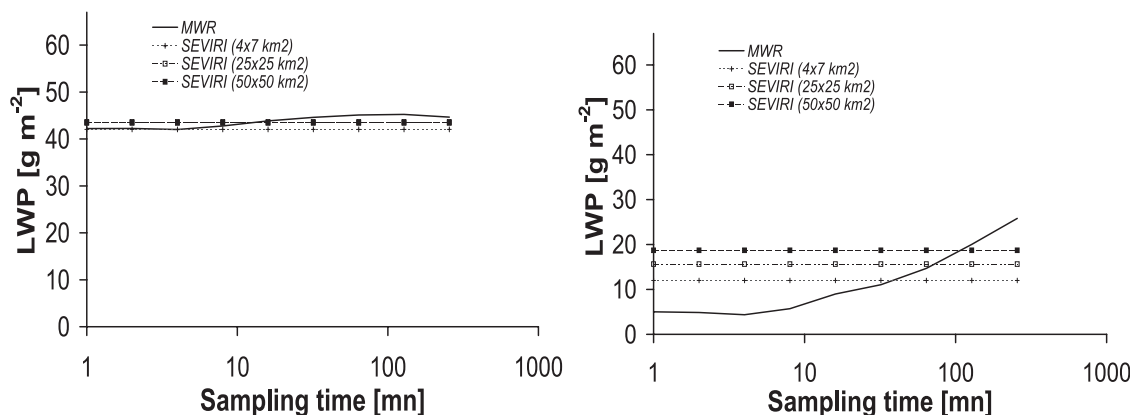


FIG. 1. (left) Mean and (right) median LWP values from MWR for sampling periods increasing from 1 to 256 min for Chilbolton during the period 15 May–30 Jun 2004. The dashed lines present the corresponding SEVIRI ($4 \times 7 \text{ km}^2$), SEVIRI ($25 \times 25 \text{ km}^2$), and SEVIRI ($50 \times 50 \text{ km}^2$) LWP values for coinciding observations over the ground-based site.

resolution and aggregated at model resolution differ by about 10 g m^{-2} . This, however, can be expected for quantities like LWP, which are lognormally distributed and skewed toward low values. Similarly, it can be seen that the MWR-calculated median LWP increases with increasing sampling time. The 32-min sampling period coincides best with the SEVIRI LWP values retrieved at satellite resolution, whereas the 64-min sampling period coincides best with the SEVIRI LWP values retrieved at the $25 \times 25 \text{ km}^2$ model resolution. These sampling periods are in agreement with the conclusions of Roebeling et al. (2006b), who found that longer sampling periods are required to represent lower-resolution grid boxes.

Figure 2 presents the distributions of LWP retrieved from MWR and SEVIRI and predicted from RACMO2 over the period from 15 May to 15 September 2004. The distributions are presented for both Cloudnet sites and for nonprecipitating water clouds and all water clouds in RACMO2. The LWP distributions from MWR, SEVIRI, and RACMO2 are lognormally distributed and have similar shapes. The tails at the low and high ends of the distributions reveal differences that can be partly attributed to sampling differences. The instantaneous sampling resolution of the MWR is about $0.1 \times 0.1 \text{ km}^2$. When Taylor's frozen turbulence hypothesis is assumed (Taylor 1938) and the wind speed is about 8 m s^{-1} , a sampling period of 64 min corresponds to a track length of about 30 km. Although the LWP values from MWR are averaged over 64 min, the MWR value corresponds to a substantially different portion of the cloud ($\sim 0.1 \times 30 \text{ km}^2$) than the model gridbox portion ($\sim 25 \times 25 \text{ km}^2$). The distribution of LWP values at Palaiseau

is dominated by thin clouds ($\text{LWP} < 25 \text{ g m}^{-2}$), which are cases with either broken cloud fields ($\sim 50\%$) or cloud free conditions ($\sim 50\%$). On the other hand, LWP values larger than 100 g m^{-2} occur very rarely in the MWR, SEVIRI, and RACMO2 data. At Chilbolton the distributions of LWP values exhibit a wider range, and a considerable fraction of the observations (about 10%) has LWP values exceeding 100 g m^{-2} . At Chilbolton the majority of the cases with LWP values $< 25 \text{ g m}^{-2}$ represents broken cloud fields ($\sim 80\%$), while only $\sim 20\%$ represents cases with cloud free conditions. The most striking feature in both distributions is that the frequency of relatively thick clouds predicted by RACMO2 is higher than observed by MWR and SEVIRI, specifically for clouds with LWP values in the range between 75 and 175 g m^{-2} .

Tables 1 and 2 provide a quantitative overview of the results for both Cloudnet sites for the observation period using four different selection conditions. It summarizes the number of observations (N), the mean LWP (LWP_{mn}), the median LWP (LWP_{50}), and the standard deviation (σLWP) of MWR- and SEVIRI-retrieved and RACMO2-predicted LWP. The four selection criteria considered are (i) cloud free and cloudy conditions, but only including nonprecipitating water clouds in RACMO2; (ii) cloudy conditions at the measurement site (cloud cover $> 80\%$), but only including nonprecipitating water clouds in RACMO2; (iii) cloud free and cloudy conditions, including all water clouds in RACMO2; and (iv) cloudy conditions at the measurement site, including all water clouds in RACMO2. The tables show that the LWP values from SEVIRI deviate, in their mean and median values, about 5 g m^{-2} from

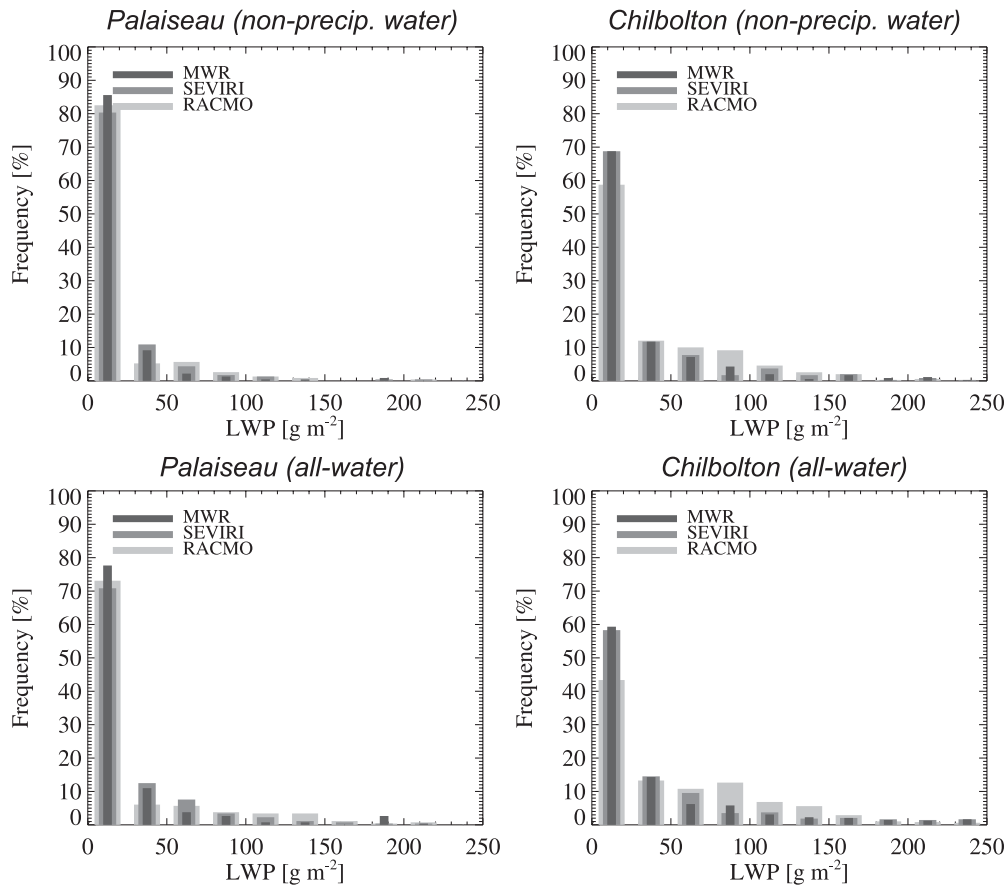


FIG. 2. Frequency distributions of observed and model-predicted LWP from MWR, SEVIRI, and RACMO2 for Chilbolton and Palaiseau during the period 15 May–15 Sep 2004, using a bin size of 25 g m^{-2} . (top) The results for nonprecipitating liquid water clouds in RACMO2 and (bottom) the results for all liquid water clouds in RACMO2.

the MWR-observed values. The RACMO2 predictions differ about 10 g m^{-2} from the MWR observations in their mean values, and about 15 g m^{-2} in their median values. It is remarkable that the RACMO2 predictions and the MWR and SEVIRI observations show similar

increases in their mean LWP values when going from “cloud free and cloudy” to “cloudy” ($\sim 40 \text{ g m}^{-2}$), or when going from “nonprecipitating clouds in RACMO2” to “all water clouds in RACMO2” ($\sim 20 \text{ g m}^{-2}$). The generally acceptable differences between

TABLE 1. Statistics of LWP values obtained from MWR and SEVIRI retrievals, and RACMO2 predictions at the Cloudnet sites of Chilbolton (CH). The statistics are calculated for four different selection conditions as described in the text, and include the number of observations (N), the mean LWP (LWP_{mn}), the median LWP (LWP_{50}), and the standard deviation of the LWP values (σLWP) during the period from 15 May to 15 Sep 2004.

	Nonprecipitating water clouds						All water clouds					
	Cloudy and cloud free $N = 349$			Cloudy $N = 99$			Cloudy and cloud free $N = 486$			Cloudy $N = 163$		
	LWP_{mn} (g m^{-2})	LWP_{50}	σLWP	LWP_{mn}	LWP_{50}	σLWP	LWP_{mn}	LWP_{50}	σLWP	LWP_{mn}	LWP_{50}	σLWP
MWR	31.0	8.0	56.7	75.9	53.3	76.1	44.2	14.4	69.2	97.8	75.8	87.9
SEVIRI	33.1	12.0	59.3	70.5	52.4	70.8	46.8	16.7	82.2	87.9	59.5	81.5
RACMO2	34.1	10.9	45.0	53.7	41.9	55.1	58.5	37.8	83.3	95.2	74.2	117.7

TABLE 2. As in Table 1, but for Palaiseau (PA), France.

	Nonprecipitating water clouds						All water clouds					
	Cloudy and cloud free <i>N</i> = 229			Cloudy <i>N</i> = 32			Cloudy and cloud free <i>N</i> = 268			Cloudy <i>N</i> = 52		
	LWP _{mn}	LWP ₅₀	σLWP	LWP _{mn}	LWP ₅₀	σLWP	LWP _{mn}	LWP ₅₀	σLWP	LWP _{mn}	LWP ₅₀	σLWP
	(g m ⁻²)			(g m ⁻²)			(g m ⁻²)			(g m ⁻²)		
MWR	11.6	2.1	25.3	47.0	34.8	48.7	20.8	4.9	42.2	72.5	41.3	70.0
SEVIRI	17.0	3.0	41.8	54.9	38.8	49.2	25.2	4.7	47.8	65.5	55.2	48.7
RACMO2	16.1	0.0	43.9	61.2	57.9	70.1	32.6	0.0	70.4	83.8	73.3	75.8

MWR- and SEVIRI-retrieved LWP values commends the SEVIRI retrievals as the appropriate data source for evaluating climate models.

5. Evaluation of the daylight cycle of RACMO2-predicted CA and CWP

The daylight cycles of CA and CWP predicted by RACMO2 are compared to corresponding cycles inferred from SEVIRI for a region covering large parts of Europe, northern Africa, and the east Atlantic (30°–60°N, 20°W–20°E). These daylight cycles are generated for the period from 15 May 2004 to 15 September 2004 using hourly cloud properties retrievals from SEVIRI and predictions from RACMO2 for solar zenith angles < 72°. Hence, the daylight cycles only include daytime information between 1 h after sunrise and 1 h before sunset. Unequal lengths in daytime period related to the north–south extent of the domain of interest and to the seasonal effect within the observation period are accounted for by sorting the data with respect to the fraction of the day, which is defined here as the normalized time between sunrise (fraction = 0) and sunset (fraction = 1). The SEVIRI-retrieved CWP values are aggregated onto the RACMO2 grid of 25 × 25 km². The CA is defined as the percentage of cloud cover within a model grid box. The SEVIRI-retrieved CA is calculated as the ratio of the cloudy and the total number of SEVIRI pixels inside the grid box. The SEVIRI-retrieved CWP values are compared to the RACMO2-predicted vertically integrated liquid water and ice sums, considering all pixels and grid boxes, including the cloud-free ones.

The daylight cycles are analyzed for the mean and the 10th (P10), 25th (P25), 50th (P50), 75th (P75), and 90th (P90) percentiles of the CA and CWP values. These values are calculated for each fraction of the day between 0.25 and 0.75. In addition, the fractions of the day that correspond to the occurrence of the daytime maximum and minimum in CA (t_{CAmax} and t_{CAmin}) and CWP (t_{CWPmax} and t_{CWPmin}), respectively, are deter-

mined by searching for their maximum and minimum values within the range of fractions of the day considered. Finally, the normalized amplitude of the daylight cycle is calculated according to

$$A = \frac{Y_{max} - Y_{min}}{Y_{max} + Y_{min}}, \quad (2)$$

where Y_{max} and Y_{min} are the daytime maximum and minimum values, respectively. This quantity measures the size of the daytime variation. To exclude daylight cycles that exhibit little variation or have too low Y_{min} values, the amplitudes and the daytime maxima and minima are only calculated when Y_{min} is greater than zero and the difference between Y_{max} and Y_{min} is greater than 10% of the daytime mean value.

a. Daylight cycles over Europe

For SEVIRI and RACMO2 Fig. 3 presents the mean values of CA and CWP over the considered domain and observation period. In general, RACMO2 predicts similar patterns of low and high CA values as SEVIRI observes. However, the magnitudes of the CA values differ notably between SEVIRI and RACMO2. Over northwestern Europe RACMO2 predicts about 20% lower CA values than SEVIRI observes. These differences are somewhat larger over land (~25%) than over the ocean (~15%). The opposite behavior is seen over the Mediterranean region where differences over land (~5%) are somewhat smaller than over sea (~10%). Note that the differences between SEVIRI and RACMO2 over the Mediterranean are generally smaller than over northwestern Europe. Over the mountains of the Picos de Europe and Pyrenees in Spain RACMO2 predicts about 15% lower CA values than SEVIRI observes, whereas over the Atlas Mountains in northwestern Africa the opposite result is found. It should be mentioned that satellite-based cloud detection algorithms are generally less reliable over mountain areas owing to frequent snow cover and large variations in surface temperature (Feijt et al. 2000). Moreover, cloud detection schemes tend to overestimate cloud

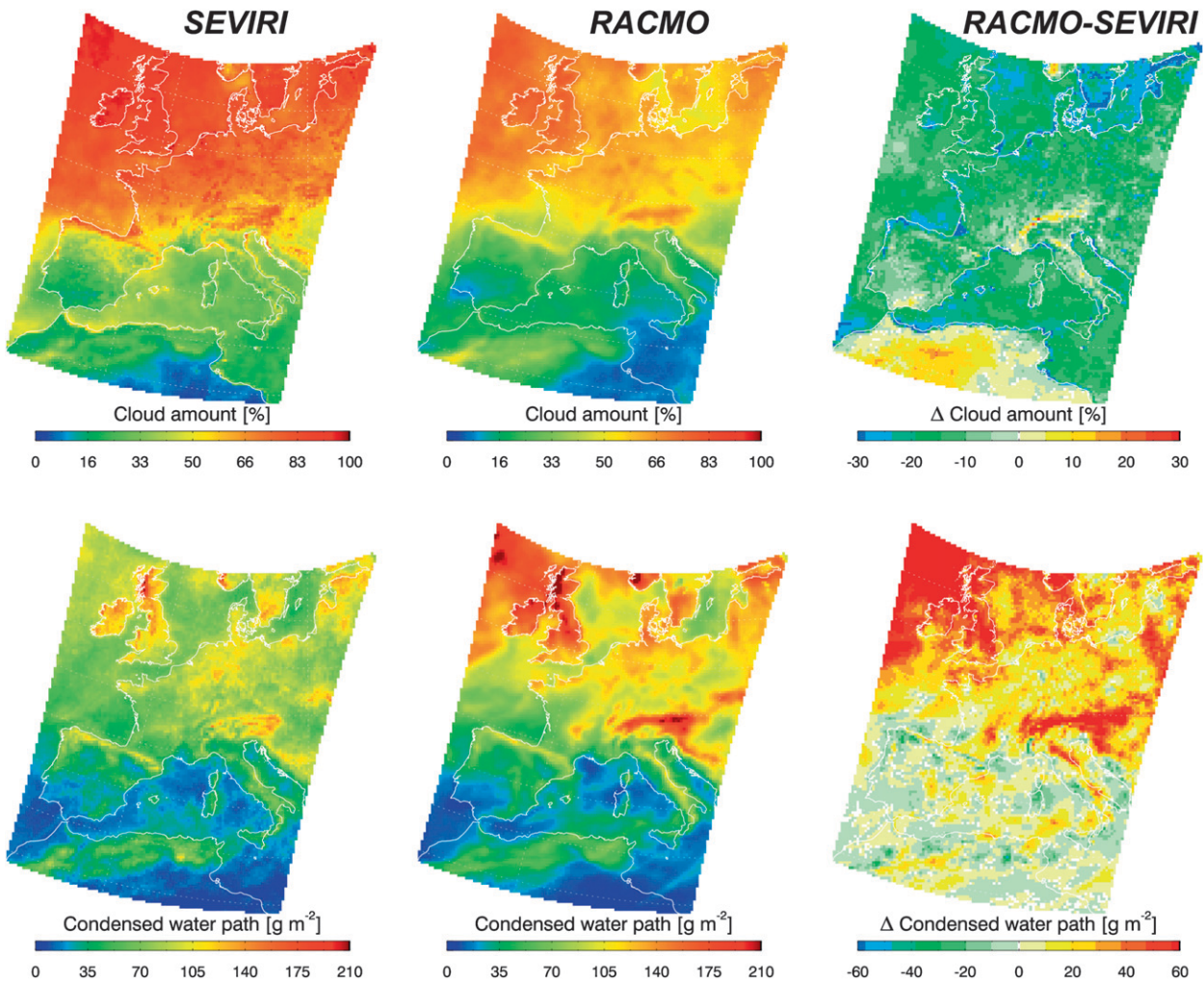


FIG. 3. Mean (top) CA and (bottom) CWP retrieved from SEVIRI and predicted by RACMO2 for Europe during the period 15 May–15 Sep 2004 using cloudy and cloud-free grid boxes. The images on the rhs present the absolute difference between RACMO2-predicted and SEVIRI-retrieved values.

amount by about 7% at viewing zenith angles $> 60^\circ$ due to the increase in the amount of cloud sides observed (Minnis 1989). Similar to the CA spatial distributions, there is good agreement between the spatial patterns of CWP from SEVIRI and RACMO2, with high CWP values over the United Kingdom, south Sweden, and the Alps and low CWP values in the Mediterranean region. However, over northern Europe the CWP values from RACMO2 and SEVIRI differ considerably in magnitude with RACMO2 predicting up to 50% larger values than retrieved by SEVIRI. The largest differences are found over the United Kingdom, Ireland, and the northern Atlantic Ocean, where CWP values from RACMO2 are up to 100 g m^{-2} larger than the SEVIRI values. A possible reason for this discrepancy is that the weather in this region is dominated by frontal systems. In such conditions RACMO2 tends to predict very large

CWP values, ranging from 150 to 250 g m^{-2} , whereas the SEVIRI-retrieved CWP ranges from 80 to 180 g m^{-2} . Note that the SEVIRI and RACMO2-inferred CWP values include both liquid and ice condensate. As mentioned in the previous section, the comparison of SEVIRI-retrieved CWP is restricted to water clouds with CWP values smaller than 800 g m^{-2} . The CWP values have not been validated for the thick cloud systems, such as over the northern Atlantic Ocean, which occasionally consist of both water droplets and ice crystals. In the Mediterranean region positive and negative differences between SEVIRI and RACMO2 are found that are generally smaller than 20 g m^{-2} over both sea and land surfaces.

Figure 4 presents the normalized amplitudes of the daylight cycles of CA and CWP values retrieved from SEVIRI and predicted from RACMO2 for the same

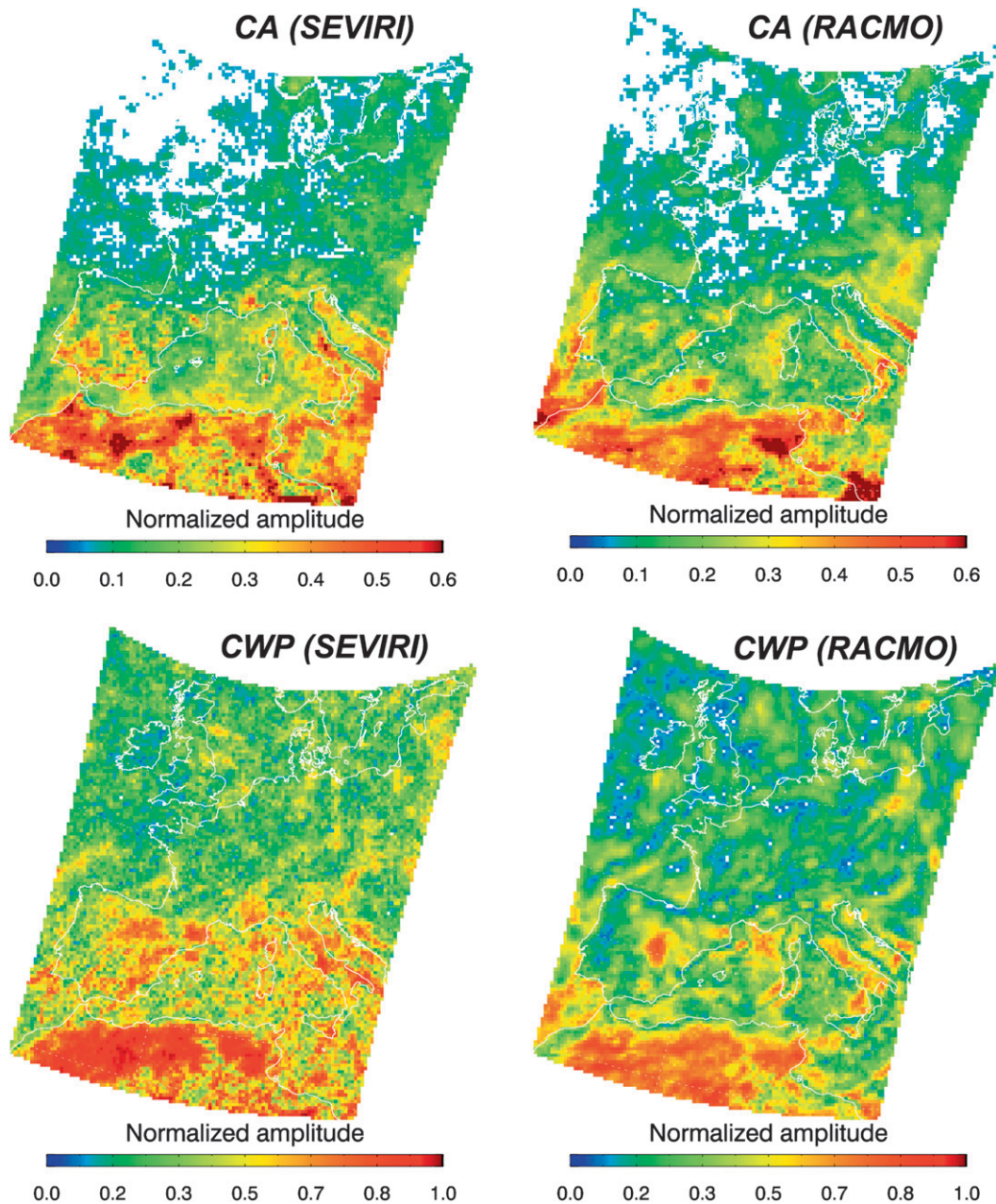


FIG. 4. Normalized amplitude of (top) CA and (bottom) CWP retrieved by SEVIRI and predicted from RACMO2 for Europe during the period 15 May–15 Sep 2004 using cloudy and cloud-free grid boxes. The white areas indicate grid boxes that exhibit little daylight variation in CA or CWP.

dataset as presented in Fig. 3. For CA the normalized amplitudes from SEVIRI and RACMO2 reveal similar spatial patterns in amplitude that show distinct variations over the study area. The largest amplitudes are seen over the land surfaces of the Mediterranean and northern Africa, where amplitudes reach values as large as 0.6. The reason for these large amplitudes is that the prevailing weather conditions in these regions in sum-

mer-time are characterized by long spells of fair weather interrupted by convective systems. For these systems, both CA and CWP from RACMO2 agree reasonably well with the SEVIRI-retrieved values. Over Spain, RACMO2 predicts somewhat smaller amplitudes in CWP than SEVIRI observes, which suggests that RACMO2 predicts weaker convection than SEVIRI observes. Over northwestern Europe the amplitudes

from SEVIRI and RACMO2 are either small (~ 0.3) or not calculated because the daylight cycle exhibits too little variations.

Figure 5 shows spatial distributions of the fraction of the day at which SEVIRI and RACMO2 values for CA and CWP reach their maximum value. The spatial distributions corresponding to CA show that there is a distinct difference between the t_{CAmax} values over land and ocean. The t_{CAmax} values over ocean are about 0.3, which corresponds to early morning maxima. Over land, maximum CA is generally found after local solar noon ($t_{CAmax} > 0.5$). However, the t_{CAmax} values over land show considerable differences between climate regions. In the Mediterranean region the t_{CAmax} values are close to 0.8 (late afternoon), whereas the t_{CAmax} values in the maritime and continental climates exhibit large regional differences and are closer to 0.5 (local solar noon). Remarkable differences are found in the transition zones between land and ocean. For example, over the sea between Italy and Croatia the t_{CAmax} values from SEVIRI are about 0.3 (early morning), whereas the t_{CAmax} values from RACMO2 are about 0.5 (afternoon). This is contrary to the differences found in the t_{CWPmax} values over this region, for which SEVIRI observes clouds to have their maximum CWP in the afternoon ($t_{CWPmax} \sim 0.7$), while RACMO2 predicts the corresponding maximum in the morning ($t_{CWPmax} \sim 0.3$). Over the Netherlands and northern Germany (maritime climate), RACMO2 predicts the largest values in CA to occur close to local solar noon or later, whereas SEVIRI observes them to occur in the early morning. This indicates that morning stratocumulus over this region is more frequently observed by SEVIRI than predicted by RACMO2. Over Spain, the t_{CWPmax} values from RACMO2 ($t_{CWPmax} \sim 0.65$) are considerably lower than from SEVIRI ($t_{CWPmax} \sim 0.75$), which indicates that maximum convection is predicted earlier by RACMO2 than is observed by SEVIRI.

b. Regional differences

To examine the daylight cycle in relation to prevailing atmospheric conditions, we focused the study on three different subdomains that are representative for three different climate zones, namely, ocean, continental, and mediterranean climates. The three subdomains are labeled the Bay of Biscay (BOB), continental Europe (CEU), and mediterranean Spain (MSP). The exact locations of the subdomains, each covering an area equivalent to 15×15 RACMO2 grid boxes (375×375 km²), are shown in Fig. 6. For each subdomain the daylight cycles of the mean and 25th and 50th percentile of SEVIRI and RACMO2-inferred CA values, and the mean and 75th and 90th percentile of SEVIRI and

RACMO2-inferred CWP are evaluated, for which the graphs are presented in Fig. 7. Likewise, for each subdomain Tables 3 and 4 list the statistics of the daylight cycle of SEVIRI and RACMO2-inferred CA and CWP values, respectively.

In the Mediterranean climate, the summertime daylight cycles of CA and CWP are dominated by convective clouds that strongly respond to the daylight cycle of the land surface temperature. During the night, the land surface cools down and convective cloud systems collapse. During the day, the surface heats up and convective processes start to develop. The strongest convection is typically found in the afternoon when surface temperatures are still high. In the MSP subdomain the daylight cycles of CA and CWP from SEVIRI and RACMO2 are very similar. Because of the low cloud amount in this area the P25 and P50 values of CA are close to zero for both SEVIRI and RACMO2. The median CWP values from SEVIRI and RACMO2 are similar and reveal the largest CWP values during late afternoon. The difference between SEVIRI-observed and RACMO2-predicted CWP values increases during the day and reach their maximum after local solar noon, when RACMO2 predicts up to 50 g m^{-2} larger CWP values than SEVIRI observes for the P90 values. Also, maximum CWP in RACMO2 is found to occur distinctly before the end of the daytime period ($t_{CWPmax} \sim 0.65$), whereas SEVIRI indicates that CWP continues to rise until at least $t_{CWPmax} = 0.75$. This finding suggests that the overestimation of CWP by RACMO2 is caused by too early onset of the convection scheme. This is consistent with the results of Lenderink et al. (2004), who found that CWP simulations from SCMs, such as RACMO2, are too active.

In the BOB subdomain, the dominating cloud type is stratocumulus for which the daylight cycle is characterized by a cloud layer that gradually thickens during the night and thins during the day owing to shortwave radiative absorption and decoupling from the surface layer (Duynkerke and Teixeira 2001). This results in distinct daylight cycles of CA and CWP that have largest values close after sunrise and smallest values close before sunset. SEVIRI and RACMO2 show very similar daylight cycles of CA and CWP for the BOB subdomain. The daylight cycles of CA have their maximum CA value during early morning and show a decrease in cloud amount during daytime. RACMO2 predicts about 5%–15% smaller CA values than those observed by SEVIRI. The largest differences are found during early morning or late afternoon. While the daylight cycles of CWP from SEVIRI and RACMO2 are very similar, the CWP values from RACMO2 are $10\text{--}20 \text{ g m}^{-2}$ larger than the corresponding values from SEVIRI. Table 4 shows that

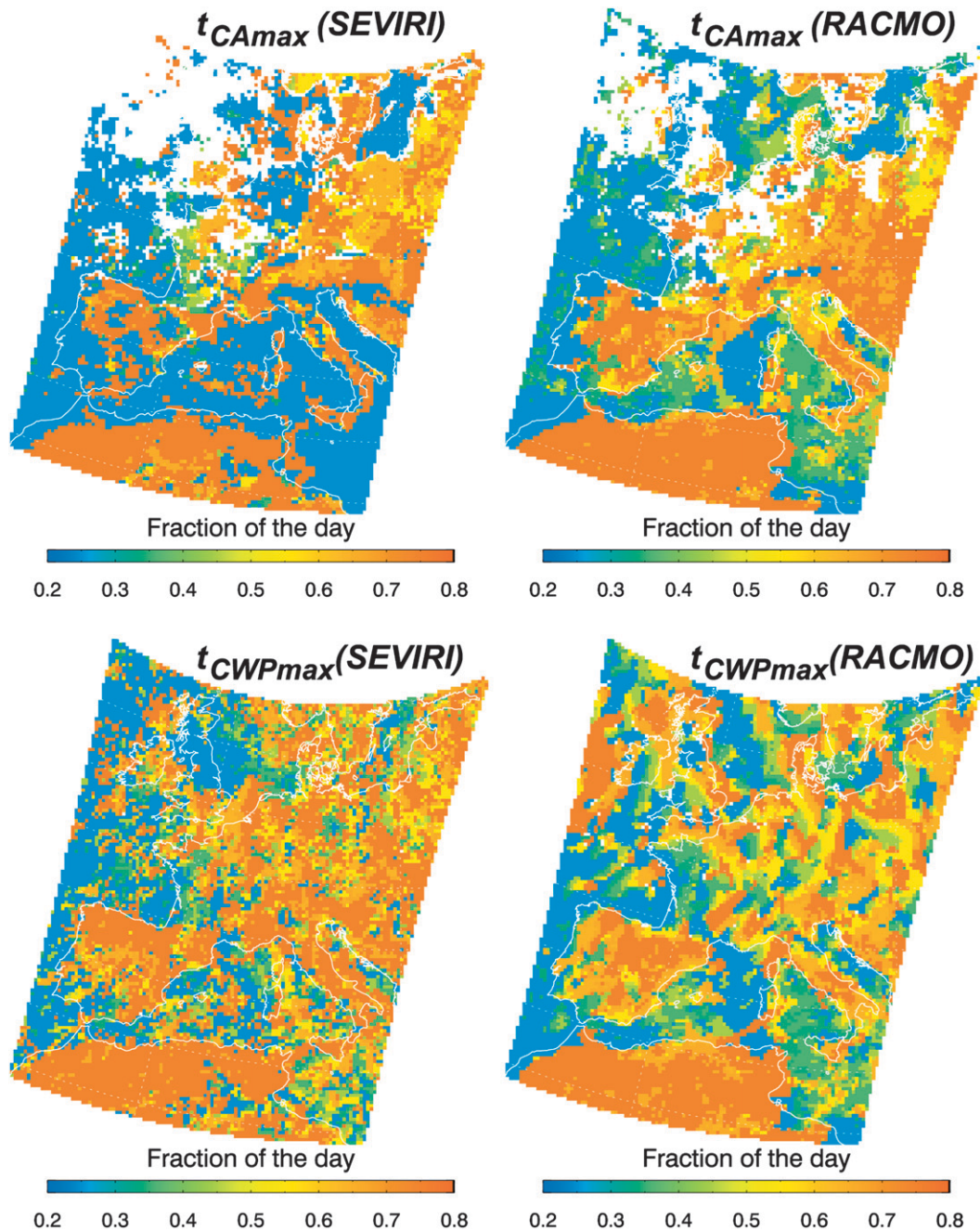


FIG. 5. The (top) t_{CAmax} and (bottom) t_{CWPmax} retrieved from SEVIRI and predicted by RACMO for Europe during the period of 15 May–15 Sep 2004 for all grid boxes. The white areas indicate grid boxes that exhibit little daylight variation in CA or CWP.

the mean CWP values from SEVIRI for the BOB subdomain are about 70 g m^{-2} , which corresponds well to the values found by Wood et al. (2002) from TMI observations ($40\text{--}80 \text{ g m}^{-2}$) or by O'Dell et al. (2008) from SSM/I, TMI, and Advanced Microwave Scanning Radiometer for Earth Observing System (EOS) (AMSR-E) observations ($50\text{--}100 \text{ g m}^{-2}$).

In the CEU subdomain, cloud systems during summer are predominantly of convective nature, whereas frontal systems occur less frequently. In general, convection over continental Europe is expected to be weaker than over the landmass of the Mediterranean region owing to the less pronounced heating of the surface during the day. On the other hand, it may be stronger because of

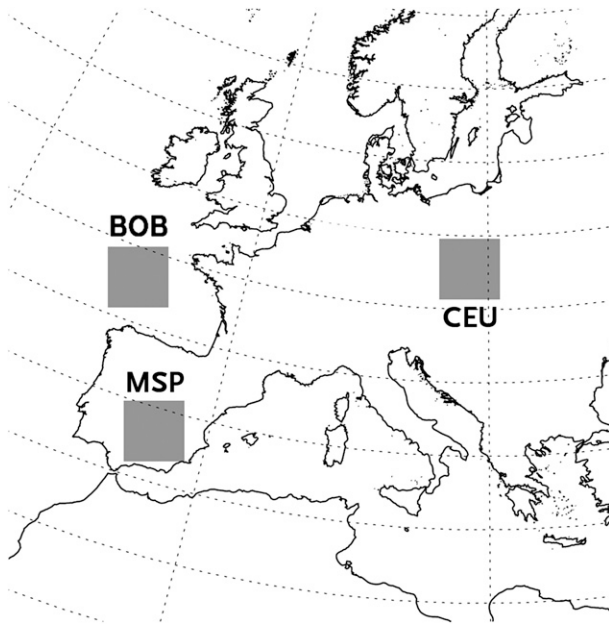


FIG. 6. Locations of the MSP, BOB, and CEU subdomains. The subdomains cover 15×15 model grid boxes ($375 \times 375 \text{ km}^2$).

the higher moisture content in the vertical profile. In the CEU subdomain the SEVIRI-inferred P25 CA value exhibits a notable daytime development with values rising from just below 20% in the morning to about 70% in the afternoon. Moreover, looking at the SEVIRI-inferred P50 CA it appears that at each instant of the daytime period it was nearly overcast during at least half of the observation period. RACMO2 exhibits similar, but less pronounced, features. In particular, the RACMO2-predicted P50 CA barely exceeds the 60% level at the end of the daytime period. Regarding CWP it is seen in Fig. 7 that in the CEU domain the thickest clouds are observed at the end of the daytime period ($t_{\text{CWPmax}} = 0.75$). This seems indicative of convection building up in the course of the day but not reaching its maximum activity before the end of the daytime period. This is contrary to the findings for the MSP subdomain where CWP associated with convection peaks before the end of the daytime period. Like for CA, RACMO2 appears capable of reproducing the daytime evolution of observed CWP. However, while the model overpredicts the P75 CWP value at all instants of the day, it tends to underestimate the CWP loading of the thickest clouds.

The general finding from all three subdomains is that RACMO2 underestimates SEVIRI-inferred CA, both at the P25 and P50 percentile, while it overpredicts the observed CWP at the P75 percentile. The exception from this apparent rule is contained in the P90 CWP, representing the 10% thickest clouds, which is either

overestimated by RACMO2 (MSP), reasonably well reproduced (BOB), or reproduced well on average but missing the observed daytime rise (CEU). It seems plausible that the inability of RACMO2 to capture the rise in P90 CWP observed in the CEU subdomain is the manifestation of shortcomings in the representation of convective processes by the model. This may also apply to the finding that RACMO2 predictions of CWP in the MSP subdomain contain a discernible daytime maximum that is not seen in the observations. This may be explained by the too early onset and too early decay of the parameterized convection in RACMO2.

6. Sensitivity to model parameters

Part of the overestimation of CWP from RACMO2 may be explained by the choice of model resolution. To analyze the effect of model resolution we intercompared RACMO2-predicted CWP values at the 25×25 and $50 \times 50 \text{ km}^2$ resolutions using the 4-month dataset over the study area. The RACMO2-predicted domain-averaged CWP value is found to decrease with about 5% in response to reducing the resolution to $50 \times 50 \text{ km}^2$, while the SEVIRI-observed CWP values are hardly affected ($< 0.5\%$) by resolution changes. We also verified the daytime CWP values from the ECMWF operational forecast, which are available at $0.5^\circ \times 0.5^\circ$ resolution for the same domain, but only at forecast times verifying at 1200 UTC. The ECMWF-predicted domain-averaged CWP values are quite comparable with RACMO2 predictions. On average, ECMWF predicts about 25% larger CWP values than SEVIRI, while RACMO2 predicts about 30% larger values at the $50 \times 50 \text{ km}^2$ resolution and about 35% at the $25 \times 25 \text{ km}^2$ resolution. The domain-averaged CWP of the operational ECMWF analysis is, averaged over the summer of 2004, about 10% less than the CWP of the successive forecasts. The accuracy of the ECMWF-predicted CWP does not depend on forecast length, but the precision decreases.

One might question the robustness of the model in representing the absolute amount of the columnar condensate water amount. With the employed setting of parameter values in the regional model physics, which is very similar to what is chosen in the original ECMWF code, the overestimation in CWP is on the order of 30%, which compares very well to what is found from the ECMWF operational forecast series. This presents a robust result in itself since it indicates that different models (GCM versus RCM, different resolutions and resolved transport) with essentially the same physics produce very similar CWP amounts. Within the physics there are quite few semiempirical parameters, the

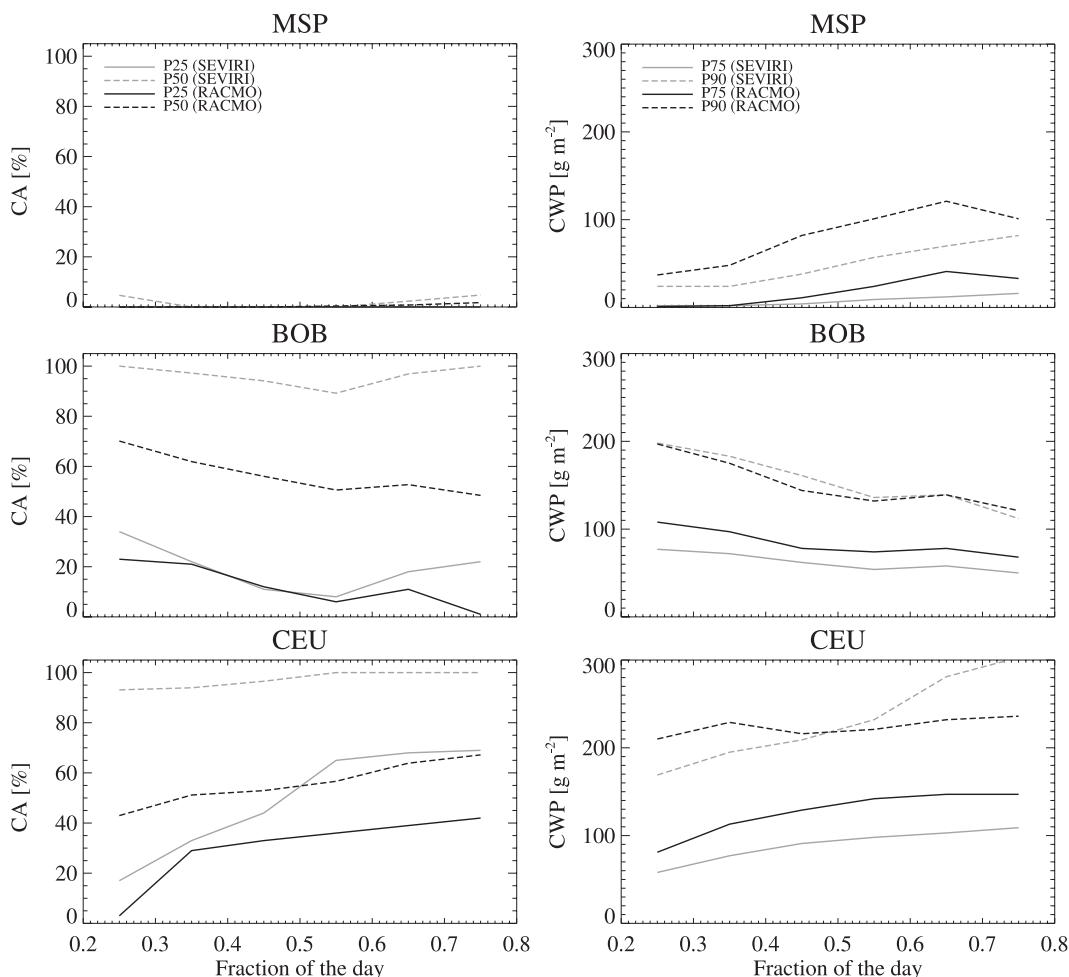


FIG. 7. Daylight cycles of SEVIRI-inferred and RACMO2-predicted 25th and 50th percentile of (left) CA values and (right) corresponding 75th and 90th percentile of CWP values for the three subdomains.

settings of which are at best inferred from observations or numerical simulations or, at worse, tuned from considerations concerning a desirable model outcome (e.g., correct sums of precipitation or right top-of-atmosphere terrestrial radiation). Many of these parameters have a minor effect to CWP amounts or no affect at all, but a few parameters potentially exert a strong affect. We have examined the role of one such parameter in more

detail. The cumulus convection scheme utilized in the ECMWF physics contains a depth parameter that acts as threshold in controlling the release of convective precipitation in relation to the thickness of the convective layer. From release cy28r1 onward, the threshold depth is set to 0 m, implying that part of the convectively produced liquid water will always be released as precipitation irrespective of the thickness of the convective

TABLE 3. Statistics of the daylight cycle of mean CA from SEVIRI and RACMO2 for MSP, BOB, and CEU subdomains during the period from 15 May to 15 Sep 2004. The statistics include the mean (\overline{CA}), the normalized amplitude (\overline{A}), and the t_{CAmax} values for the mean, P25, and P50.

Region	SEVIRI					RACMO2				
	\overline{CA} (%)	\overline{A}	t_{CAmax} mean	t_{CAmax} P25	t_{CAmax} P50	\overline{CA} (%)	\overline{A}	t_{CAmax} mean	t_{CAmax} P25	t_{CAmax} P50
MSP	26	0.19	0.75	-	-	23	0.18	0.75	-	-
BOB	66	0.07	0.25	0.25	0.25	56	0.10	0.25	0.25	0.25
CEU	74	0.11	0.75	0.75	0.75	58	0.14	0.75	0.75	0.75

TABLE 4. As in Table 2, but for the statistics of the daylight cycle of mean CWP from SEVIRI and RACMO2. The statistics include the mean ($\overline{\text{CWP}}$), the normalized amplitude (\overline{A}), and the t_{CWPmax} values for the mean, P75, and P90.

Region	SEVIRI					RACMO2				
	$\overline{\text{CWP}}$ (g m^{-2})	\overline{A} (-)	t_{CWPmax} mean	t_{CWPmax} P75	t_{CWPmax} P90	$\overline{\text{CWP}}$ (g m^{-2})	\overline{A} (-)	t_{CWPmax} mean	t_{CWPmax} P75	t_{CWPmax} P90
MSP	29	0.49	0.75	0.75	0.75	26	0.36	0.64	0.66	0.64
BOB	62	0.30	0.25	0.25	0.25	72	0.24	0.25	0.25	0.25
CEU	88	0.31	0.75	0.75	0.75	117	0.16	0.75	0.66	0.75

layer. In the version of RACMO2.1 applied to multi-annual climate-type integrations (E. van Meijgaard et al. 2008), the threshold depth has been set to a physically more sound value of 1500 m, implying that the release of precipitation is suppressed for, generally speaking, the case of shallow convection. The consequence of enhancing the threshold depth parameter is primarily a suppression of convective precipitation. Although this effect is partly compensated by an increase in stratiform (also referred to as large scale) precipitation, the net result is that total precipitation decreases (total is sum of convective and large-scale contributions). This is illustrated in Fig. 8a, which shows the total precipitation accumulated from model events with precipitation rates between zero and a given value. A second consequence is a suppression of events with low precipitation in the convective precipitation rate as illustrated by Fig. 8c. Metaphorically speaking, a constantly dripping tap turns into an intermittently bursting tap. For the purpose of the regional model in climate-type integrations this change has resulted in a meaningful improvement. It is found from comparing model frequency distributions of daily precipitation amounts with observations from the Rhine catchment that the regional model version with enhanced threshold depth parameter is better capable of representing the frequency of extreme amounts of precipitation. This outcome is illustrated in Fig. 8b. A third consequence, which is of particular relevance to this study, is that the frequency distribution of CWP, as shown in Fig. 8d, shifts toward higher values because the conversion of cloud water into precipitation is delayed, or even inhibited. As a result, the quasi-steady-state amount of columnar condensate water shifts to a larger value. In fact, it is found that the impact of modifying the threshold depth is rather drastic. An integration with RACMO2 at 25 km, carrying the alternatively set parameter, results in the overprediction of CWP to rise from 35% to 80%. Similarly, at 50-km resolution, the overprediction is found to grow from 30% to about 55% (not shown). Interestingly, the enhancement of the CWP amounts are found rather evenly distributed across the entire domain and not restricted to regions that are

dominated by convection. This seems to indicate that, within the context of the model, the suppression of convective precipitation when convection is transporting moisture upward results in an excess moisture source for cloud formation in the prognostic cloud scheme. This process is not restricted to grid columns with convective activity, but also spreads to columns downstream, owing to resolved-scale transport of condensed water. Finally, the enhancement of CWP is accompanied by an increase in cloud amount, but this is found to be marginally small.

7. Discussion and conclusions

This paper presents the evaluation of daylight cycles of cloud amount (CA) and condensed water path (CWP) predicted in the Regional Climate Model version 2 (RACMO2) with *Meteosat-8*-based SEVIRI observations. By virtue of the use of SEVIRI observations, this evaluation could be performed, for the first time, over both land and ocean surfaces. The utilization of SEVIRI-inferred CWP for the evaluation of predictions made with a (regional) climate model is justified by comparing SEVIRI LWP retrievals with collocated and synchronous observations with microwave radiometers made at two Cloudnet sites.

The LWP values retrieved from SEVIRI and predicted from RACMO2 have been compared with a statistically significant sample of LWP observations from MWR at two Cloudnet sites. This comparison shows that the SEVIRI-retrieved LWP values have a higher accuracy ($\sim 5 \text{ g m}^{-2}$) than the corresponding accuracy obtained from RACMO2 predictions ($\sim 15 \text{ g m}^{-2}$). It should be mentioned that the comparison results are only applicable for water clouds with LWP values lower than 800 g m^{-2} , which includes more than 95% of the water clouds. Moreover, the quality of cloud water path retrievals for mixed phase clouds or ice clouds is uncertain due to lack of reliable observations. In the near future ice water path retrievals of cirrus clouds may be validated with Cloudsat and Calipso observations, using the combined lidar and radar ice water path retrievals algorithm of Donovan and van Lammeren (2001). However, for thick ice

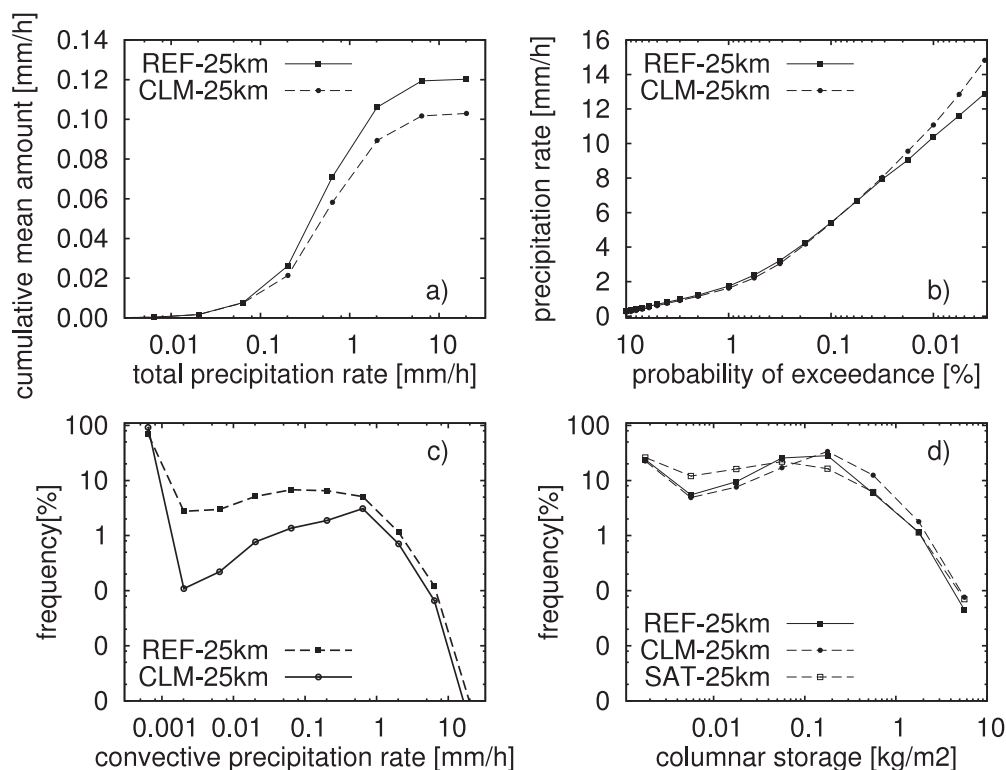


FIG. 8. (a) Total model precipitation (see text for explanation of the phrase “total”) accumulated from model events with precipitation rates between zero and a given value as inferred from RACMO2 at grid box level for the reference run (REF) and the sensitivity run (CLM), both operated at 25-km resolution, and (b) the hourly precipitation rates that are exceeded at a given probability. (c) The frequency distribution of hourly rates of precipitation generated in the convection scheme, and (d) the frequency distribution of CWP at gridbox level. The SAT-labeled curve in (d) refers to the SEVIRI-inferred CWP values aggregate model resolution. To gain statistics this analysis is carried out for a rectangular domain of 30×30 RACMO grid cells over central Europe.

clouds or mixed phase clouds, such as deep convective systems or multiple-layer cloud systems, validation will remain very difficult.

The model evaluation yields as the primary finding that RACMO2 operated at 25-km resolution predicts, when averaged over the full domain and entire observation period, about 35% larger CWP values and 20% lower CA values than retrieved with SEVIRI. The effect of horizontal resolution is small; a model run at 50-km resolution reduces the overestimation of CWP to 30%. On the other hand, the model-predicted CWP is found very sensitive to variations in a threshold depth parameter that controls the conversion of cloud liquid water into rain within the parameterized convection. An unrealistic setting of this parameter permitting this conversion to happen at any convective depth leads to the best results as discussed so far. A more realistic setting of this parameter, such that the process of conversion is inhibited when the convective depth is less than a prescribed threshold, results in a considerable

increase of columnar water amount. Adopting this parameter setting was motivated by the finding that it improved the representation of extreme precipitation events in climate integrations with RACMO2; however, this study reveals that it has further enhanced the overestimation of columnar water amounts. This result seems to indicate that the source terms of cloud water content in the RACMO2 physics are too productive. Other aspects of CWP, such as spatial distribution and temporal evolution, are found to be marginally sensitive to variations in the threshold depth parameter.

Geographically viewed, contributions to the overprediction of CWP are predominantly coming from the northwest portion of the domain, including Ireland and the British Isles, where frontal conditions with stratiform clouds prevail, and from land areas with significant orography. An exception is formed by the Spanish Picos de Europe and the Pyrenees where CWP are reasonably well represented by the model. Regarding cloud amount, RACMO2 is found to underpredict SEVIRI

values across the large part of the domain, with deviations up to 30% in southern Sweden and in coastal areas of the North Sea and Baltic Sea. On the other hand, CA is consistently overestimated in most areas of northern Africa, the southeast of France, and in some regions with significant orography. The irradiance differences in the radiation scheme of RACMO2 will be partly compensated owing to the overestimation of CWP and the simultaneous underestimation of CA relative to SEVIRI. This compensation might have a completely different effect on the radiation scheme of RACMO2 in a changing climate where the clouds thickness changes. For example, a thickening of clouds would lead to a negligible reduction of irradiance in the RACMO2 predictions, whereas it would lead to a significant irradiance reduction in the SEVIRI observations. Also, since the analysis of the daylight cycle shows that the highest daytime CA values are found close to local solar noon or slightly later, an increase in CWP might have a stronger cooling effect than anticipated by the climate model.

Despite the differences in absolute amount, the spatial variations in the normalized amplitude and the daytime fraction of occurrence of the largest CA and CWP values as retrieved by SEVIRI and predicted by RACMO2 are found to compare reasonably well. The largest normalized amplitudes are found in the Mediterranean region, where the values are about 0.4 for CA and about 0.7 for CWP. The daytime fractions at which the largest CA and CWP values occur differ considerably over the different climate zones, with early morning maxima of CA and CWP over oceans and late noon maxima over Mediterranean land. The $t_{CA_{max}}$ and $t_{CWP_{max}}$ values observed from SEVIRI and predicted from RACMO2 are found to differ most in the coastal regions or in regions with diverse weather conditions, for example, around Italy or the Netherlands. In the case of variable weather conditions, RACMO2 has to switch frequently between different physical parameterization schemes, for example, between the stratiform and the shallow or deep convection schemes, which poses a model challenge.

The comparison over the selected subdomains reveals that RACMO2 predicts maximum convection about 3 h after local solar noon ($0.65 < t_{CWP_{max}} < 0.75$) for the subdomains in continental Europe and in Spain, while SEVIRI always observes these maxima around sunset ($t_{CWP_{max}} > 0.75$). The daylight cycles of CWP from SEVIRI and RACMO2 correspond best for the Bay of Biscay subdomain, where the $t_{CWP_{max}}$ values are about 0.25 and 0.50, respectively. However, for these regions CA values from SEVIRI are considerably larger than the corresponding RACMO2 values, with the largest differences during early morning and late afternoon observations.

In conclusion, this study shows that the satellite-retrieved daylight cycle of cloud properties provides a powerful tool in identifying strengths and weaknesses in the representation of cloud parameters by climate models. With four years of SEVIRI data now available, the evaluation of daylight cycles can be extended to include additional seasons and different years. Such study might further contribute to our understanding of cloud-related processes and their interaction with large-scale dynamics and land surface processes.

Acknowledgments. This work was part of the EUMETSAT-funded Climate Monitoring Satellite Application Facility project. Further, we wish to thank Arnout Feijt, Piet Stammes, Hartwig Deneke, and Erwin Wolters for reviewing earlier versions of this manuscript. We also thank Jérôme Riédi for providing the SEVIRI cloud-detection code. Finally, we acknowledge the Cloudnet project (European Union Contract EVK2-2000-00611) for providing the microwave radiometer data, which was produced by the University of Reading using measurements from the Chilbolton Facility for Atmospheric and Radio Research, part of the Rutherford Appleton Laboratory and SIRTa, operated by the Institut Pierre Simon Laplace (IPSL).

REFERENCES

- Ackerman, S. A., K. I. Strabala, W. P. Menzel, R. A. Frey, C. C. Moeller, and L. E. Gumley, 1998: Discriminating clear sky from clouds with MODIS. *J. Geophys. Res.*, **103**, 32 141–32 157.
- Curry, J. A., and Coauthors, 2000: FIRE Arctic Clouds Experiment. *Bull. Amer. Meteor. Soc.*, **81**, 5–29.
- de Bruijn, C., and E. van Meijgaard, 2005: Verification of HIRLAM with ECMWF physics compared with HIRLAM reference versions. HIRLAM Tech. Rep. 63, 39 pp.
- De Haan, J. F., P. B. Bosma, and J. W. Hovenier, 1987: The adding method for multiple scattering calculations of polarized light. *Astron. Astrophys.*, **183**, 371–391.
- Donovan, D. P., 2003: Ice-cloud effective particle size parameterization based on combined lidar, radar reflectivity, and mean Doppler velocity measurements. *J. Geophys. Res.*, **108**, 4573, doi:10.1029/2003JD003469.
- , and A. C. A. P. van Lammeren, 2001: Cloud effective particle size and water content profile retrievals using combined lidar and radar observations. 1. Theory and simulations. *J. Geophys. Res.*, **106**, 27 425–27 448.
- Duynkerke, P. G., and J. Teixeira, 2001: Comparison of the ECMWF reanalysis with FIRE I observations: Diurnal variation of marine stratocumulus. *J. Climate*, **14**, 1466–1478.
- , and Coauthors, 2004: Observations and numerical simulations of the diurnal cycle of the EUROCS stratocumulus case. *Quart. J. Roy. Meteor. Soc.*, **130**, 3269–3296, doi:10.1256/qj.03.139.
- Fairall, C. W., J. E. Hare, and J. B. Snider, 1990: An eight-month sample of marine stratocumulus cloud fraction, albedo, and integrated liquid water. *J. Climate*, **3**, 847–864.

- Feijt, A., P. de Valk, and S. van der Veen, 2000: Cloud detection using Meteosat imagery and numerical weather prediction model data. *J. Appl. Meteor.*, **39**, 1017–1030.
- Gaussiat, N., R. J. Hogan, and A. J. Illingworth, 2007: Accurate liquid water path retrieval from low-cost microwave radiometers using additional information from lidar and operational forecast models. *J. Atmos. Oceanic Technol.*, **24**, 1562–1575.
- Greenwald, T. J., and S. A. Christopher, 1999: Daytime variation of marine stratocumulus microphysical properties as observed from geostationary satellite. *Geophys. Res. Lett.*, **26**, 1723–1726.
- Han, Q., W. B. Rossow, R. Welch, A. White, and J. Chou, 1995: Validation of satellite retrievals of cloud microphysics and liquid water path using observations from FIRE. *J. Atmos. Sci.*, **52**, 4183–4195.
- Hess, M., R. B. A. Koelemeijer, and P. Stammes, 1998: Scattering matrices of imperfect hexagonal ice crystals. *J. Quant. Spectrosc. Radiat. Transfer*, **60**, 301–308.
- Hogan, R. J., M. P. Mittermaier, and A. J. Illingworth, 2006: The retrieval of ice water content from radar reflectivity factor and temperature and its use in evaluating a mesoscale model. *J. Appl. Meteor. Climatol.*, **45**, 301–317.
- Illingworth, A. J., and Coauthors, 2007: Cloudnet: Continuous evaluation of cloud profiles in seven operational models using ground-based observations. *Bull. Amer. Meteor. Soc.*, **88**, 883–898.
- Jakob, C., and A. P. Siebesma, 2003: A new subcloud model for mass-flux convection schemes: Influence on triggering, updraft properties, and model climate. *Mon. Wea. Rev.*, **131**, 2765–2778.
- Jolivet, D., and A. J. Feijt, 2005: Quantification of the accuracy of liquid water path fields derived from NOAA 16 advanced very high resolution radiometer over three ground stations using microwave radiometers. *J. Geophys. Res.*, **110**, D11204, doi:10.1029/2004JD005205.
- King, M. D., S. Platnick, P. Yang, G. T. Arnold, M. A. Gray, J. C. Riedi, S. A. Ackerman, and K.-N. Liou, 2004: Remote sensing of liquid water and ice cloud optical thickness, and effective radius in the Arctic: Application of airborne multispectral MAS data. *J. Atmos. Oceanic Technol.*, **21**, 857–875.
- Lenderink, G., B. van den Hurk, E. van Meijgaard, A. P. van Ulden, and J. Cuijpers, 2003: Simulation of present-day climate in RACMO2: First results and model developments. KNMI Tech. Rep. 252, 24 pp.
- , and Coauthors, 2004: The diurnal cycle of shallow cumulus clouds over land: A single-column model intercomparison study. *Quart. J. Roy. Meteor. Soc.*, **130**, 3339–3364.
- Minnis, P., 1989: Viewing zenith angle dependence of cloudiness determined from coincident GOES East and GOES West data. *J. Geophys. Res.*, **94** (D2), 2303–2320.
- Nakajima, T. Y., and T. Nakajima, 1995: Wide-area determination of cloud microphysical properties from NOAA AVHRR measurements for the FIRE and ASTEX regions. *J. Atmos. Sci.*, **52**, 4043–4059.
- O'Dell, C. W., F. J. Wentz, and R. Bennartz, 2008: Cloud liquid water path from satellite-based passive microwave observations: A new climatology over the global oceans. *J. Climate*, **21**, 1721–1739.
- Platnick, S., M. D. King, S. A. Ackerman, W. P. Menzel, B. A. Baum, J. C. Riedi, and R. A. Frey, 2003: The MODIS cloud products: Algorithms and examples from Terra. *IEEE Trans. Geosci. Remote Sens.*, **41**, 459–473.
- Ramaswamy, V., and Coauthors, 2001: Radiative forcing of climate change. *Climate Change 2001: The Scientific Basis*, J. T. Houghton et al., Eds., Cambridge University Press, 349–416.
- Roebeling, R. A., A. J. Feijt, and P. Stammes, 2006a: Cloud property retrievals for climate monitoring: Implications of differences between Spinning Enhanced Visible and Infrared Imager (SEVIRI) on METEOSAT-8 and Advanced Very High Resolution Radiometer (AVHRR) on NOAA-17. *J. Geophys. Res.*, **111**, D20210, doi:10.1029/2005JD006990.
- , N. A. J. Schutgens, and A. J. Feijt, 2006b: Analysis of uncertainties in SEVIRI cloud property retrievals for climate monitoring. Preprints, *12th Conf. on Atmospheric Radiation*, Madison, WI, Amer. Meteor. Soc., P4.51. [Available online at <http://ams.confex.com/ams/pdfpapers/112865.pdf>.]
- , H. M. Deneke, and A. J. Feijt, 2008: Validation of cloud liquid water path retrievals from SEVIRI using one year of CloudNET observations. *J. Appl. Meteor. Climatol.*, **47**, 206–222.
- Rossow, W. B., and B. Cairns, 1995: Monitoring changes of clouds. *Climatic Change*, **31**, 175–217.
- , and R. A. Schiffer, 1999: Advances in understanding clouds from ISCCP. *Bull. Amer. Meteor. Soc.*, **80**, 2261–2287.
- Stammes, P., 2001: Spectral radiance modeling in the UV-visible range. *IRS 2000: Current Problems in Atmospheric Radiation*, W. L. Smith and Y. M. Timofeyev, Eds., A. Deepak, 385–388.
- Stephens, G. L., G. W. Paltridge, and C. M. R. Platt, 1978: Radiation profiles in extended water clouds. III: Observations. *J. Atmos. Sci.*, **35**, 2133–2141.
- Taylor, G. I., 1938: The spectrum of turbulence. *Proc. Roy. Soc. London*, **132A**, 476–490.
- Uppala, S. M., and Coauthors, 2005: The ERA-40 Re-Analysis. *Quart. J. Roy. Meteor. Soc.*, **131**, 2961–3012.
- van Meijgaard, E., and S. Crewell, 2005: Comparison of model predicted liquid water path with ground-based measurements during CLIWA-NET. *Atmos. Res.*, **75**, 201–226.
- , L. H. van Ulft, W. J. van de Berg, F. C. Bosveld, B. J. J. M. van den Hurk, G. Lenderink, and A. P. Siebesma, 2008: The KNMI regional atmospheric climate model RACMO, version 2.1. KNMI Tech. Rep. 302, 43 pp.
- van Zadelhoff, G.-J., A. J. Heymsfield, D. P. Donovan, and M. J. McGill, 2007: Evaluating lidar–radar microphysics retrieval using in situ measurements. *J. Geophys. Res.*, **112**, D09213, doi:10.1029/2006JD007202.
- Weng, F., N. C. Grody, R. R. Ferraro, A. Basist, and D. Forsyth, 1997: Cloud liquid water climatology from the special sensor microwave imager. *J. Climate*, **10**, 1086–1096.
- White, P. W., Ed., 2003: Physical processes. ECMWF IFS documentation cycle CY23r4, 166 pp. [Available online at http://www.ecmwf.int/research/ifsdocs_old/pdf_files/Physics.pdf.]
- Wolters, E. L. A., R. A. Roebeling, and A. J. Feijt, 2008: Evaluation of cloud-phase retrieval methods for SEVIRI on Meteosat-8 using ground-based lidar and cloud radar data. *J. Appl. Meteor. Climatol.*, **47**, 1723–1738.
- Wood, R., C. S. Bretherton, and D. L. Hartmann, 2002: Diurnal cycle of liquid water path over the subtropical and tropical oceans. *Geophys. Res. Lett.*, **29**, 2092, doi:10.1029/2002GL015371.